Hindawi
Mathematical Problems in Engineering
Volume 2021, Article ID 6691941, 10 pages
https://doi.org/10.1155/2021/6691941

*Research Article*

# Fractional-Order Hyperbolic Tangent Sliding Mode Control for Chaotic Oscillation in Power System

**Darui Zhu**,[1] **Wenchao Zhang**,[2] **Chongxin Liu**,[3] **and Jiandong Duan**[1]

[1]*School of Electrical Engineering, Xi'an University of Technology, Xi'an 710048, China*
[2]*School of Water Resources and Hydroelectric Engineering, Xi'an University of Technology, Xi'an 710048, China*
[3]*School of Electrical Engineering, Xi'an Jiaotong University, Xi'an 710049, China*

Correspondence should be addressed to Jiandong Duan; duanjd@xaut.edu.cn

Received 30 December 2020; Revised 2 April 2021; Accepted 22 April 2021; Published 13 May 2021

Academic Editor: Junyong Zhai



Chaotic oscillation will occur in power system when there exist periodic load disturbances. In order to analyze the chaotic oscillation characteristics and suppression method, this paper establishes the simplified mathematical model of the interconnected two-machine power system and analyzes the nonlinear dynamic behaviors, such as phase diagram, dissipation, bifurcation map, power spectrum, and Lyapunov exponents. Based on fractional calculus and sliding mode control theory, the fractional-order hyperbolic tangent sliding mode control is proposed to realize the chaotic oscillation control of the power system. Numerical simulation results show that the proposed method can not only suppresses the chaotic oscillation but also reduce the convergence time and suppress the chattering phenomenon and has strong robustness.

## 1. Introduction

With the increasing scale of power system, the nonlinear characteristics are more complex in power systems. Chaotic oscillation and even blackouts will occur in power system due to a number of reasons, such as periodic load disturbances, parameter variation, voltage collapse, frequency collapse, and transient instability [1–5]. How to effectively control chaos in the power system has become a common problem to be considered both theoretically and practically. Chaotic oscillation is an important phenomenon that has attracted considerable attention in recent years. The mechanism causing chaotic oscillation is described and the difference between chaotic oscillation and loss of stability is distinguished [6]. The nonlinear dynamic characteristics of a simple three-bus power system mathematic model are studied, including phase diagrams and a bifurcation map [7]. Reference [8] proposed a conventional power network system and demonstrated the chaotic behavior under some special operating conditions. The reasons for chaos in the power system have been investigated employing the theory of nonlinear dynamic systems based on a simple power system model. The critical conditions and parameter region in which chaos occurs have been worked out using the Melnikov function calculation method [9]. Based on the fractional calculus, [10] reported the dynamic analysis of a fractional-order power system and established its numerical simulations which are provided to demonstrate the feasibility and efficacy of the analysis.

Based on the above analysis of the chaotic oscillation mechanism in power system, there are two aspects to suppress the chaotic oscillation: one is controlling the system's behavior to the expected orbit and the other is suppressing the occurrence of the chaotic oscillations in power system. In recent years, various nonlinear control strategies have been applied to chaos control in power systems, such as LS-SVM method [11], the finite-time stability theory method [12], ANFIS method [13], adaptive control method [14–17], and sliding mode control method [18–26]. In a practical application, the sliding mode control (SMC) has the advantages of a fast dynamic response, good stability, and strong antidisturbance ability, and it is widely used in many control systems. The main problem hindering the engineering application of the conventional sliding mode control

is the well-known chattering phenomenon. In order to solve the chattering problem of SMC, [22] proposed an equivalent fuzzy fast terminal sliding mode control method, and this method can not only reduce the chattering but also accelerate the convergence time. In order to reduce chattering phenomenon of SMC, [23] designed a sliding mode observer to suppress the chaotic oscillation in power system by using the hyperbolic tangent function instead of the symbolic function. Reference [24] presented a fast fixed-time nonsingular terminal sliding mode control method to suppress chaotic oscillation in power systems, and the proposed control scheme achieved system stabilization within bounded time independent of initial condition and has an advantage in convergence rate over existing result of fixed-time stable control method. Based on fixed-time stability theory, [25] designed a fixed-time integral sliding mode controller to ensure the precise convergence of the state variables of controlled system and overcame the drawback of convergence time growing unboundedly as the initial value increases in finite time controller. Reference [26] proposed a new adaptive fuzzy sliding mode control design strategy for the control of a special class of three-dimensional fractional-order chaotic systems with uncertainties and external disturbance. The design methodology is developed in two stages: first, an adaptive sliding mode control law is proposed for the class of fractional-order chaotic systems without uncertainties, and then a fuzzy logic system is used to estimate the control compensation effort to be added in the case of uncertainties on the system's model.

All of the above references are designed by using integer-order sliding mode controllers, but the fractional-order sliding mode control increases two control freedom degrees and makes the controller design more flexibility. In recent years, fractional-order sliding mode control has been applied to other fields and has better control result. Reference [27] proposed a novel optimized fractional-order controller for control of chaos in power system and discussed the steps to optimize the order of fractional controller. The proposed controller perturbed the dynamics of the nonlinear power system and pushed it to nonchaotic and bounded stable state. Reference [28] proposed a novel discrete-time fractional-order sliding mode control scheme which guarantees the desired tracking performance of a linear motor control system; and a better performance is achieved due to the memory effect of the fractional calculus. Reference [29] proposed a fractional-order sliding mode control strategy for grid-connected doubly fed induction generator. The simulation results fully exhibited the effectiveness of the proposed method and indicated that the fractional-order sliding mode control strategy has superior performance over that of the conventional sliding mode control scheme. As the contributions to the fractional-order sliding mode control investigation efforts, [30] proposed a new adaptation law for fractional-order sliding mode control addressing the synchronization problem for a class of nonlinear fractional-order systems with chaotic behavior. The main innovation in the proposed control design concerns the choice of a sliding surface with two adjustable parameters, leading easily to an efficient adaptation law for the sliding mode control controller. Therefore, the design of sliding mode controller using fractional calculus theory can suppress the chaotic oscillation in power system effectively.

The rest of this paper is organized as follows. System description and the basic chaotic oscillation characteristics are analyzed in Section 2 and Section 3, respectively. Section 4 gives some mathematical preliminaries. In Section 5, the fractional-order hyperbolic tangent sliding mode controller is proposed to suppress the chaotic oscillation in power system, and the theoretical analysis and proof are given. Section 6 gives the comparison of the proposed controller with the traditional sliding mode controllers. Conclusions end the paper in Section 7.

## 2. System Description

Reference [9] presented a dual-unit power system that consists of generator, transformer, transmission line, and power load. By simplifying the presented exact model, the second-order mathematical model of the interconnected two-machine power system is obtained, which is shown in Figure 1.

In Figure 1, 1 and 2 are the equivalent generators; 3 and 4 are the equivalent transformers of systems S1 and S2, respectively. 5 is power load, 6 is the circuit breaker, and 7 is the transmission line. According to the analysis of the above interconnected two-machine power system, we can get the second-order mathematical model, which is shown as follows:

$$\begin{cases} \dfrac{\mathrm{d}\delta}{\mathrm{d}t} = \omega, \\ \dfrac{\mathrm{d}\omega}{\mathrm{d}t} = -\dfrac{1}{H}P_s \sin\,\delta - \dfrac{D}{H}\omega + \dfrac{1}{H}P_m + \dfrac{1}{H}P_e \cos\,t, \end{cases} \tag{1}$$

where $\delta$ is the electrical angle between generators 1 and 2, $\omega$ is the corresponding relative angle speed, $H$ is the equivalent moment inertia of S1, $P_S$ is electromagnetic power of generator 1, $P_m$ is mechanical power of the generator 2, $D$ is the damping coefficient, and $P_e \cos\,t$ is disturbance of S1.

Here, let $a = (1/H)P_s, b = (D/H), e = (P_m/H), F = (P_e/H), x_1 = \delta, x_2 = \omega$.

Equation (1) can be simplified as follows:

$$\begin{cases} \dfrac{\mathrm{d}x_1}{\mathrm{d}t} = x_2, \\ \dfrac{\mathrm{d}x_2}{\mathrm{d}t} = -a\,\sin\,x_1 - bx_2 + e + F\,\cos\,t. \end{cases} \tag{2}$$

When $a = 1, b = 0.02, e = 0.2, F = 0.2593$, chaotic oscillation will occur in the power system, and the corresponding system parameters of system (1) are $H = 100\ \mathrm{kg\,m^2}$, $P_s = 100\mathrm{W}$, $D = 2\ \mathrm{N\,m\,s/rad}$, $P_m = 20\ \mathrm{W}$, and $P_e = 25.93\ \mathrm{W}$. The time-domain waveforms and phase diagram of system (1) are shown in Figures 2 and 3, respectively.

As can be seen from Figures 2 and 3, it is known that the dynamic behavior of the power system is complex. It appears that chaotic oscillation is accompanied by voltage instability

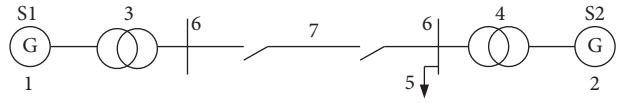


Figure 1: The interconnected two-machine power system.

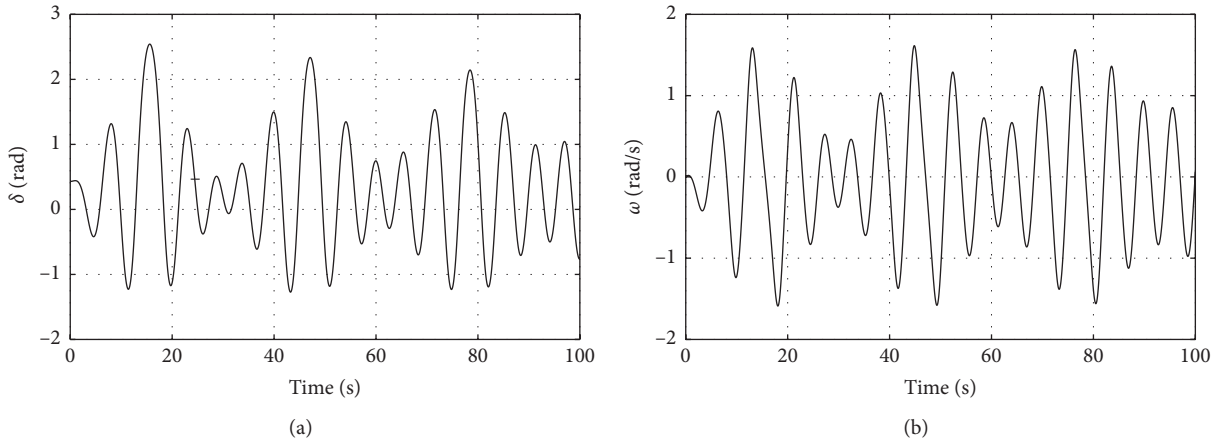


Figure 2: Time-domain waveform of system (1). (a) Time-domain waveform of $\delta$. (b) Time-domain waveform of $\omega$.

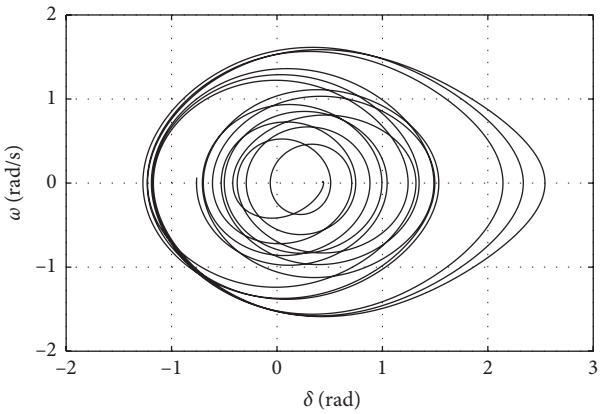


Figure 3: Chaotic attractor phase diagram.

and frequency oscillation under the above parameter conditions. The existence of chaos and chaos control of the interconnected two-machine power system will be investigated to suppress chaotic oscillation.

## 3. Basic Characteristics

*3.1. Dissipative Analysis.* By calculation, the divergence of system (1) can be obtained:

$$\nabla V = \frac{\partial \dot{\delta}}{\partial \delta} + \frac{\partial \dot{w}}{\partial w} = -0.02 < 0, \tag{3}$$

and, from equation (3), we can get that system (1) is dissipative, and the trajectory is bounded and converged in the exponential form $(dV/dt) = e^{-(D/H)t}$. In other words, the initial volume element $V_0$ converges to $V_0 e^{-(D/H)t}$ at $t$. When $t \longrightarrow \infty$, the trajectories of each volume element will converge to zero according to the exponential rate $-(D/H)$. That is, all trajectories would be restricted to the zero volume set and fixed on an attractor. Thus, chaotic attractor exists in system (1).

*3.2. Lyapunov Exponent.* The Lyapunov exponents of a chaotic trajectory have at least one positive value, which corresponds to the sensitive dependence feature. This feature distinguishes a strange attractor from the other types of steady-state behaviors. By calculation, the computation Lyapunov exponents are LE1 = 0.0174, LE2 = 0, and LE3 = −0.0374 at $P_m = 20$W. System (1) is a chaotic system with the positive Lyapunov exponent [31, 32]. The mechanical power $P_m$ has a great influence on stable operation in power system with excitation limitation, which determines the speed of the generator. To better understand the dynamics of power system (1), the Lyapunov exponents with the parameter $P_m$ are shown in Figure 4. As can be seen, when the mechanical power $P_m$ is located in (17.38, 55.1), (56.25, 7.15), (69.9, 76), (80.34, 80.68), and (81.32, 100), the largest Lyapunov exponent of system (1) is larger than zero, and the system is chaotic.

*3.3. Bifurcation Diagram.* Power system is a complex nonlinear dynamic system; bifurcation phenomenon will occur with the changes of parameters. Bifurcation is the main route to chaos from the stable state, and it will cause the system to lose stability. The bifurcation map is used to analyze the dynamic characteristics of the nonlinear system when the system parameter varies [33]. It is known that the system parameter disturbance power amplitude $P_e$ must change all the time and the system conditions can change when the system is disturbed by inevitable disturbances. Thus, the bifurcation map is shown in Figure 5 with the disturbance power amplitude $P_e$ varying. From the

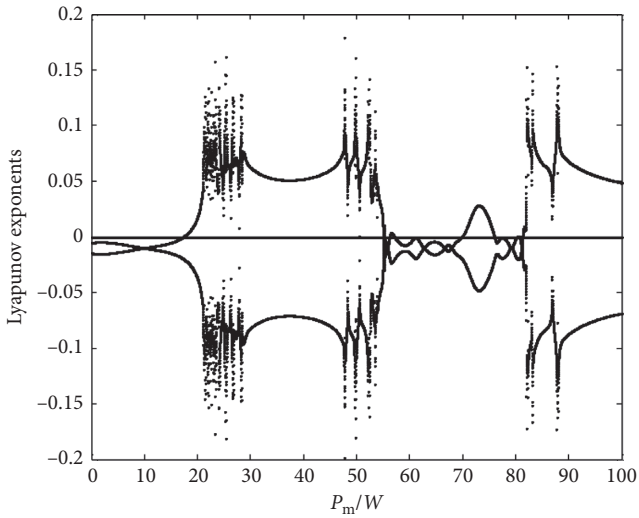


Figure 4: Lyapunov exponents.

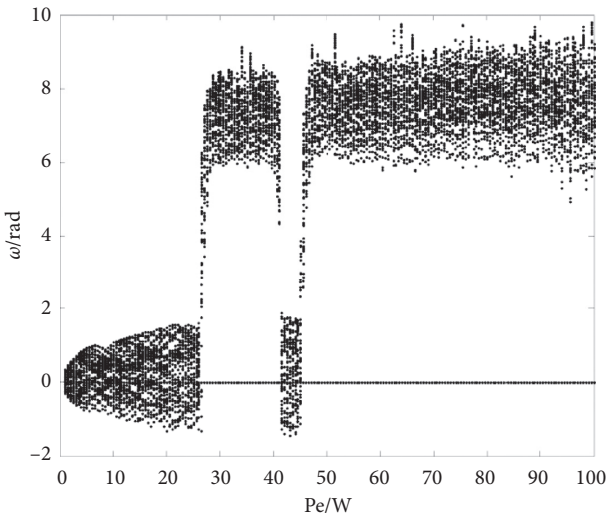


Figure 5: Bifurcation map of $P_e$.

bifurcation map in Figure 5, we can see that chaotic oscillation will occur in the system when the disturbance power amplitude $P_e$ is under some certain condition.

*3.4. Power Spectrum.* Chaotic oscillation is the nonperiodic motion; its power spectrum is continuous and there will appear a new crossover or multiplier peak frequency in bifurcation processing. The power spectrum of system (1) could be calculated and analyzed by the following indirect method.

First, the autocorrelation function of the sample data should be calculated as follows:

$$R_x(\tau) = E\{x(t)x(t+\tau)\} = \lim_{T\longrightarrow\infty} \frac{1}{T}\int_0^T x(t)x(t+\tau)\mathrm{d}t. \tag{4}$$

Then, the power spectrum is obtained by the Fourier transform for autocorrelation function, and it is shown in Figure 6. From the simulation results, the power spectrum of system (1) is a continuous spectral line without obvious peak value. Thus, chaotic oscillation occurs in system (1).

## 4. Mathematical Preliminaries

At present, there are several definitions of the fractional-order differential systems. Two commonly used definitions are Grünwald–Letnikov (GL) definition and Riemann-Liouville (RL) definition.

The best-known RL definition of fractional-order system can be expressed as [34]

$$\frac{\mathrm{d}^q f(t)}{\mathrm{d}t^q} = \frac{1}{\Gamma(n-q)}\frac{\mathrm{d}^n}{\mathrm{d}t^n}\int_0^t \frac{f(\tau)}{(t-\tau)^{q-n+1}}\mathrm{d}\tau, \tag{5}$$

where $n$ is an integer value satisfying $n-1 \le q < n$, and $\Gamma(\cdot)$ is the $\Gamma$-function.

Consider a general fractional-order nonlinear dynamical system as follows:

$$D^q X = f(X) \text{ or } D^q X = AX, \tag{6}$$

where $X \in R^n (\in N)$, $A \in R^{n\times n}$, $0 < q \le 1$.

**Lemma 1.** *For a given autonomous linear system of fractional-order system (6) with $x(0) = x_0$, where $x(t) \in R^n$ is the state vector, from [35], we know the following:*

*(1) The system is asymptotically stable if and only if $|\arg(\lambda_i(A))| > (\alpha\pi/2), i = 1, 2, \ldots, n$, where $\arg(\lambda_i(A))$ denotes the argument of the eigenvalues $\lambda_i$ of $A$*

*(2) The system is stable if and only if either it is asymptotically stable or those critical eigenvalues satisfying $|\arg(\lambda_i(A))| = (\alpha\pi/2)$ have geometric multiplicity of one*

**Lemma 2** (see [36, 37]). *For the nonlinear fractional-order system (6) with the order of $0 < q \le 1$, if there exists a real symmetric positive definite matrix $P$ satisfying $J(t) = X^T(t)PD^qX(t) \le 0$, where $X(t) = (x_1(t), x_2(t), \ldots, x_n(t))$, then system (6) is asymptotically locally stable.*

**Lemma 3** (see [38]). *When $\varepsilon > 0$, for any value $\chi \in R$ and a constant $\varepsilon > 0$, there is an inequality that is established in the following:*

$$0 \le |\chi| - \chi \tanh\left(\frac{\chi}{\varepsilon}\right) \le \mu\varepsilon, \mu = 0.2785, \tag{7}$$

**Lemma 4** (see [30]). *Let $x = 0$ be a point of equilibrium for the fractional-order system $D^\alpha x(t) = f(x,t)$, where $f(x,t)$ is Lipschitz with a Lipschitz constant $l > 0$ and $\alpha \in (0,1)$. Suppose that there exists a Lyapunov function $V(t, x(t))$ such that*

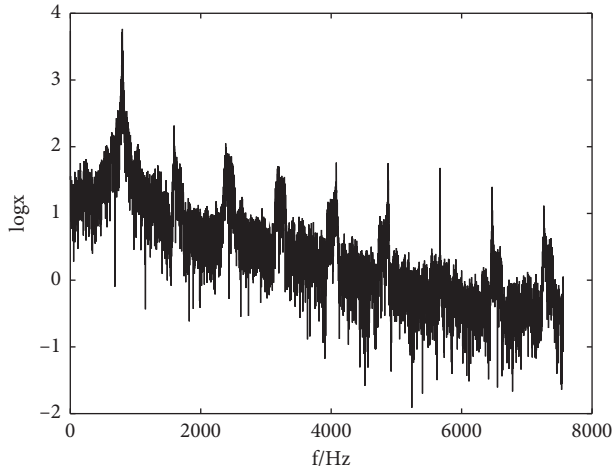


Figure 6: Power spectrum of system (1).

$$\begin{cases} a_1\|x\|^b \le V(t,x) \le a_2\|x\|, \\ \dot{V}(t,x) \le -a_3\|x\|, \end{cases} \tag{8}$$

*where $a_1$, $a_2$, $a_3$, and $b$ are positive constants. Then the equilibrium point of the fractional-order system is Mittag–Leffler (asymptotically) stable.*

**Lemma 5** (see [39]). *For a continuous system,*

$$\begin{cases} \dot{x} = f(x) \\ f(0) = 0 \end{cases}, \quad x \in R^n. \tag{9}$$

If there is a continuous positive definite function $V\colon R^n \longrightarrow R$ and there exists a neighborhood $U_0 \subseteq R^n$ of the origin point satisfying (10), system (9) is globally finite time stable.

$$\dot{V}(x) + aV^{\alpha}(x) \le 0, \quad x \in \frac{U_0}{\{0\}}, \tag{10}$$

where $a \in R^+$, $0 < \alpha < 1$.

## 5. Controller Design

To eliminate chaotic oscillation in power system (1), a sliding mode controller is proposed to keep the power system operating on a stable motion. The simplified controlled system is described as follows:

$$\begin{cases} \dfrac{dx_1(t)}{dt} = x_2(t), \\ \dfrac{dx_2(t)}{dt} = f(x(t)) + d(t) + u(t), \end{cases} \tag{11}$$

where $f(x(t)) = -a \sin x_1(t) - bx_2(t) + e$, $d(t) = F\cos t$, and $u(t)$ is the designed sliding mode controller. Assume that the uncertain perturbation term is bounded that $|d(t)| \le F$, where $F$ is a positive constant.

*5.1. Design of the Sliding Mode Controller.* First, $x_d(t)$ is the control input of the interconnected two-machine power system (1), the error is defined as $e(t) = x_1(t) - x_d(t)$, and the sliding mode switching function is designed as follows:

$$s(t) = ce(t) + \dot{e}(t), \tag{12}$$

where $c$ should satisfy Hurwitz condition, that is, $c > 0$; then

$$\begin{aligned} s(t) &= c\dot{e}(t) + \ddot{x}_1(t) - \ddot{x}_d(t) = c\dot{e}(t) + \ddot{x}_2(t) - \ddot{x}_d(t) \\ &= c\dot{e}(t) - \ddot{x}_d(t) + [f(x(t)) + d(t) + u(t)]. \end{aligned} \tag{13}$$

The controller $u(t)$ can be designed as $u(t) = u_{\text{eq}}(t) + u_{\text{sw}}(t)$ based on sliding mode control theory; and the equivalent controller $u_{\text{eq}}(t)$ can be obtained by $\dot{s}(t) = 0$, where

$$u_{\text{eq}}(t) = \ddot{x}_d(t) - c\dot{e}(t) - f(x(t)). \tag{14}$$

The switching controller is designed as

$$u_{\text{sw}}(t) = -\eta s(t) - F\,\text{sgn}(s(t)). \tag{15}$$

Then, the sliding mode controller $u(t)$ becomes

$$u(t) = \ddot{x}_d(t) - c\dot{e}(t) - f(x(t)) - \eta s(t) - F\,\text{sgn}(s(t)). \tag{16}$$

Lyapunov function is designed as $V_S(t) = 0.5s^2(t)$; thus,

$$\dot{V}_s(t) = s(t)\dot{s}(t) = s(t)[c\dot{e}(t) + (f(x(t)) + d(t) + u(t)) - \ddot{x}_d(t)]. \tag{17}$$

Substitute (14) into (15), and we can obtain

$$\begin{aligned} \dot{V}_s(t) &= s(t)\dot{s}(t) = s(t)[c\dot{e}(t) - (f(x(t)) + d(t) + u(t)) + \ddot{x}_d(t)] \\ &= s(t)[d(t) - F\text{sgn}(s(t)) - \eta s(t) \\ &= s(t)d(t) - F|s(t)| - \eta s^2(t). \end{aligned} \tag{18}$$

The disturbance satisfied condition $|d(t)| \le F$; thus $\dot{V}_s(t) = s(t)\dot{s}(t) \le 0$. In other words, the Lyapunov function

satisfied that $V_s(t)$ is positive definite and $\dot{V}_s(t)$ is semi-negative definite. The system is stable.

*5.2. Design of the Fractional-Order Hyperbolic Tangent Sliding Mode Controller.* Because switching function is discontinuous in traditional sliding mode control, it may cause the unexpected chattering phenomenon in actual controller design. Compared with the traditional switching function, the continuous smooth hyperbolic tangent function can soften the controller output characteristic and the fractional-order controller can make the system have better performance. Thus, the fractional-order sliding surface and hyperbolic tangent sliding control law are designed to reduce the chattering in sliding mode control.

The fractional-order sliding mode function is designed as follows:

$$\begin{aligned} s(t) &= ce(t) + \dot{e}(t) + D^{\alpha}e(t) \\ \dot{s}(t) &= c\dot{e}(t) + f(x) + u(t) + d(t) - \ddot{x}_d(t) + D^{\alpha+1}e(t). \end{aligned} \tag{19}$$

The controller $u(t)$ can be designed as $u(t) = u_{\text{eq}}(t) + u_{\text{sw}}(t)$. The fractional-order equivalent controller $u_{\text{eq}}(t)$ can be obtained by $\dot{s}(t) = 0$, where

$$u_{\text{eq}}(t) = \ddot{x}_d(t) - c\dot{e}(t) - f(x) - D^{\alpha+1}e(t). \tag{20}$$

The hyperbolic tangent switching controller $u_{\text{sw}}(t)$ is designed:

$$u_{\text{sw}}(t) = -\eta s(t) - F \tanh\left(\frac{s(t)}{\varepsilon}\right). \tag{21}$$

Then, the controller $u(t)$ becomes

$$u(t) = \left(\ddot{x}_d(t) - c\dot{e}(t) - f(x) - D^{\alpha+1}e(t) - \eta s(t) - F \tanh\left(\frac{s(t)}{\varepsilon}\right)\right). \tag{22}$$

According to Lemma 3, it can be obtained that

$$|s(t)| - s(t)\tanh\left(\frac{s(t)}{\varepsilon}\right) \le \mu\varepsilon. \tag{23}$$

That is, $F|s(t)| - Fs(t)\tanh(s(t)/\varepsilon) \le F\mu\varepsilon$. It satisfies

$$-Fs(t)\tanh\left(\frac{s(t)}{\varepsilon}\right) \le -F|s(t)| + F\mu\varepsilon. \tag{24}$$

It can be obtained that

$$\begin{aligned} \dot{V}(t) &= s^T(t)\dot{s}(t) \\ &= s^T(t)\left(c\dot{e}(t) + f(x) + u(t) + d(t) - \ddot{x}_d(t) + D^{\alpha+1}e(t)\right) \\ &= s^T(t)\left(d(t) - \eta s(t) - KD^{\alpha-1}\tanh\left(\frac{s(t)}{\varepsilon}\right)\right) \\ &\le s^T(t)d(t) - \eta s^T(t)s(t) - Ks(t). \end{aligned} \tag{25}$$

Based on $d(t) \le K$, (25) can be written in the following form:

$$\begin{aligned} \dot{V}(t) &\le s^T(t)d(t) - \eta s^T(t)s(t) - Ks(t)_1 \\ &\le -K - \eta s^T(t)s(t) \\ &\le -K - \eta(2V(t))^{(1/2)}. \end{aligned} \tag{26}$$

We can get $\dot{V}(t) + \eta(2V(t))^{(1/2)} \le -K$; that is,

$$\dot{V}(t) + \eta(2V(t))^{(1/2)} \le 0. \tag{27}$$

According to the above analysis and combining fractional stability in Lemmas 4 and 5, we can obtain that the system is globally finite time stable with fractional-order sliding mode controller and $\lim_{t\to\infty} e(t) = \dot{e}(t) = 0$. The stability of the controller is verified.

## 6. Numerical Simulation

In order to verify the control effect of the proposed control method, the fractional-order hyperbolic tangent sliding mode controller is established by MATLAB/Simulink. Selecting the system parameters as $a = 1$, $b = 0.02$, $e = 0.2$, and $F = 0.2593$, the tracking target is $x_d = \sin t$, the controller parameters are designed as $c = 25$, $K = 2$, $\eta = 20$, and $\varepsilon = 0.02$, and the fractional-order parameter is chosen as $\alpha = 0.8$. Simulation time is set as 10 s, and the fractional-order hyperbolic tangent sliding mode controller is added to system (11). Simulation results of the time-domain waveform are shown in Figure 7, and the corresponding error waveforms are shown in Figure 8. In order to compare with the control effect between the designed controllers, simulation results of the traditional sliding model control, the hyperbolic tangent sliding mode control, and the fractional-order hyperbolic tangent sliding mode control are shown in Figures 9–11, respectively [40].

Compared with the above simulation results, we can get the following:

(1) From Figures 7 and 8, it can be seen that the chaotic interconnected two-machine power system is restored to the expected state when the designed fractional-order hyperbolic tangent sliding mode controller is added to the chaotic system. Simulation results show that the power system stability is realized, and the chaotic oscillation is suppressed effectively by the proposed controller.

(2) By comparing with the simulation results in Figures 9 and 10, the chattering phenomenon is reduced by the continuous smooth hyperbolic tangent functions, and the system control performance is further improved by the proposed fractional-order sliding surface. By calculation in Figure 10, the angle speed relative errors of the three different sliding mode control are 0.91%, 0.626%, and 0.21%.

(3) Compared with the results of the controller output in Figure 11, it can be seen that the continuous smooth hyperbolic tangent function can soften the controller output performance; and the fractional-order sliding

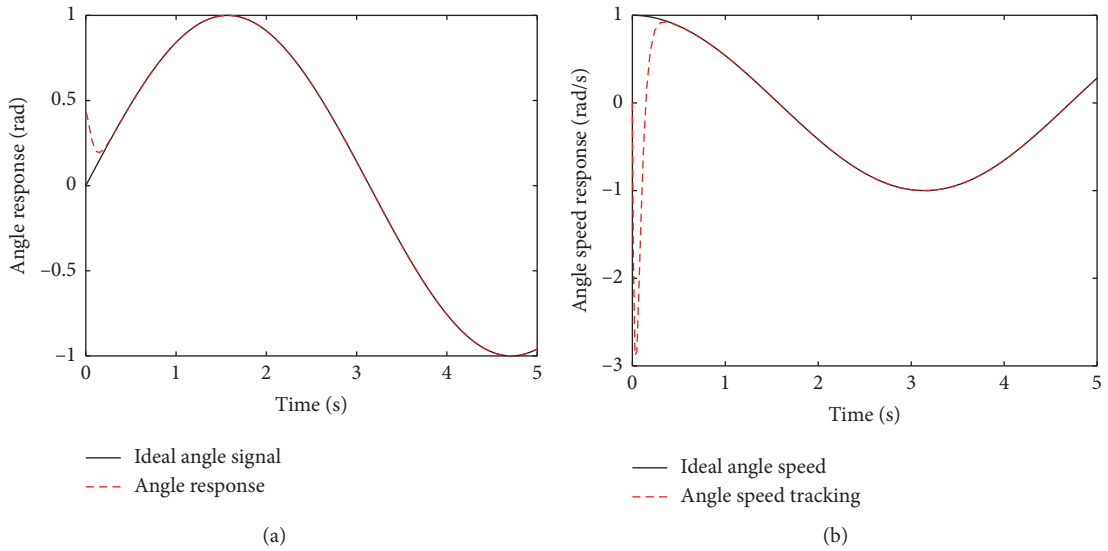


Figure 7: Time-domain waveforms under the designed controller. (a) Time-domain waveform of $\delta$. (b) Time-domain waveform of $\omega$.

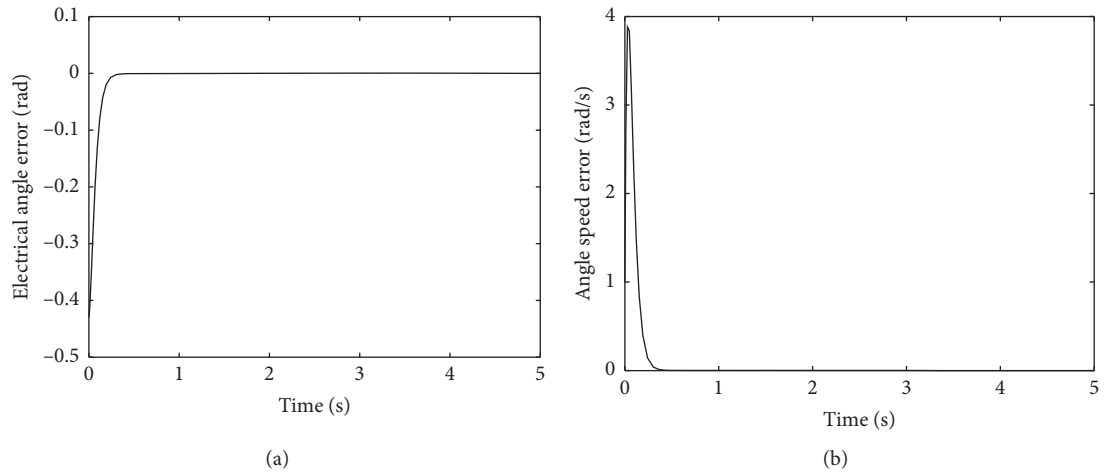


Figure 8: Error waveform under the designed controller. (a) Error waveform of $\delta$. (b) Error waveform of $\omega$.

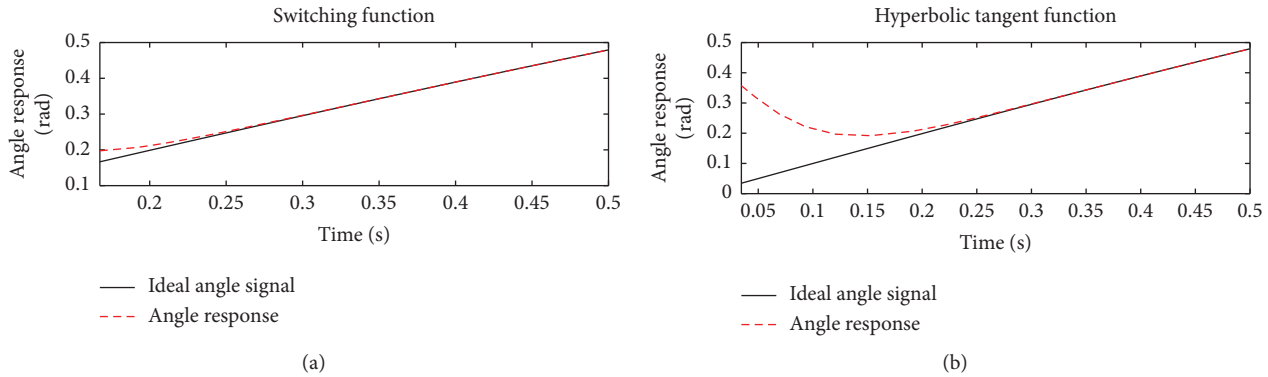


Figure 9: Continued.

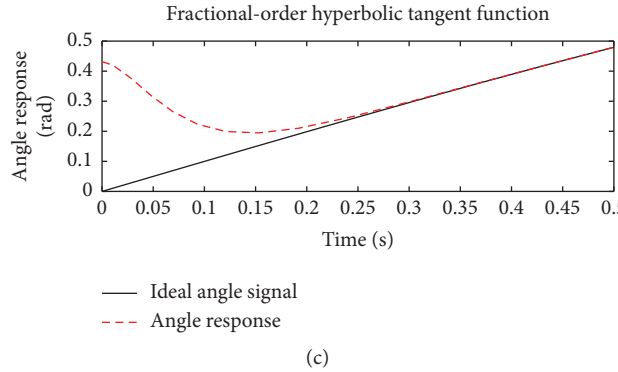


Figure 9: Partial enlargements of the time-domain waveform $\delta$.

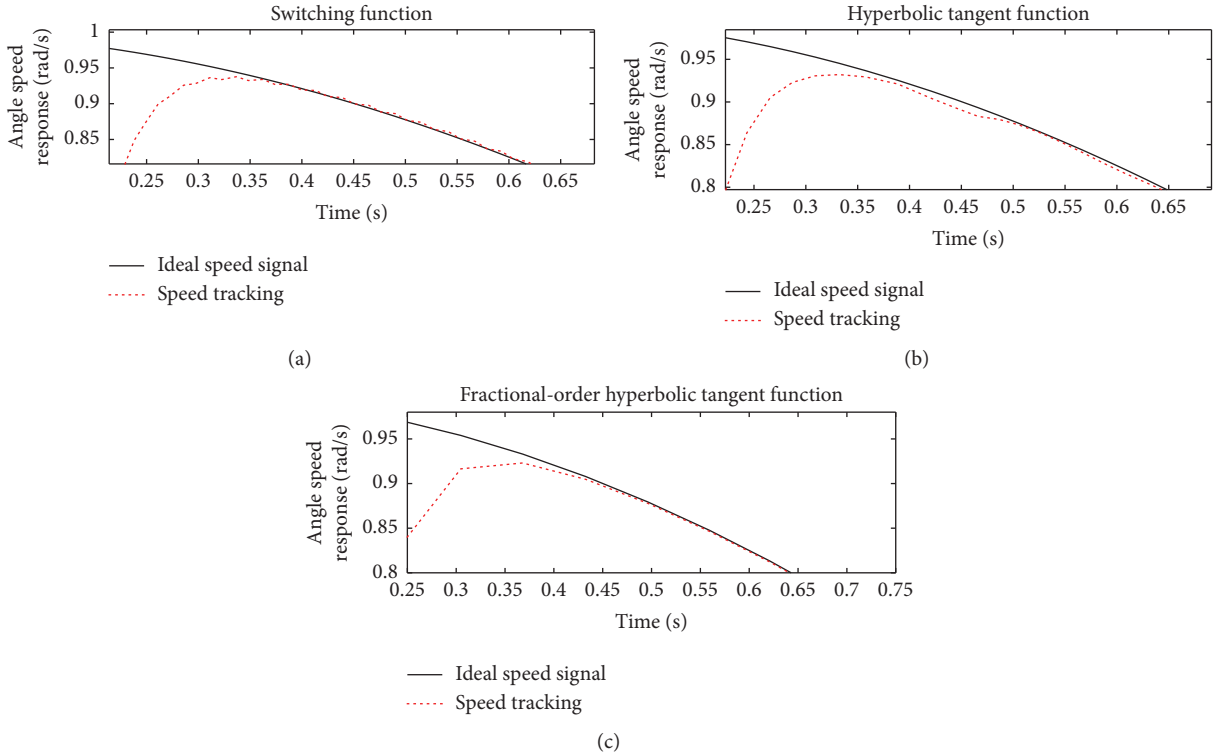


Figure 10: Partial enlargements of the time-domain waveform $\omega$.

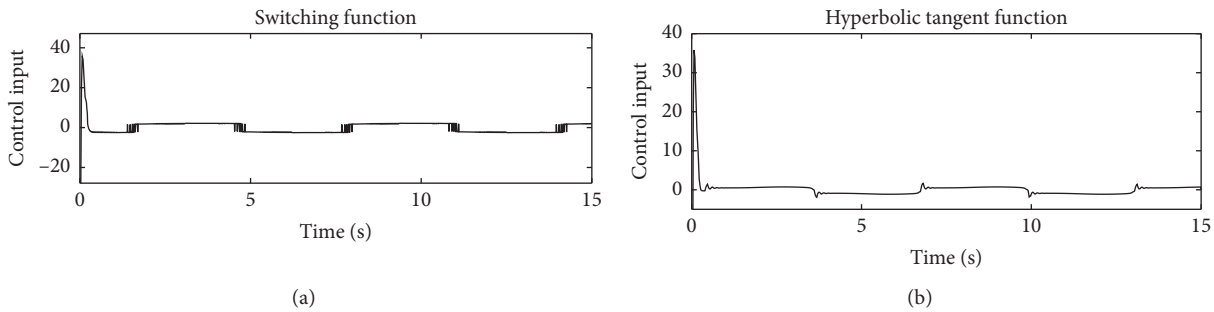


Figure 11: Continued.

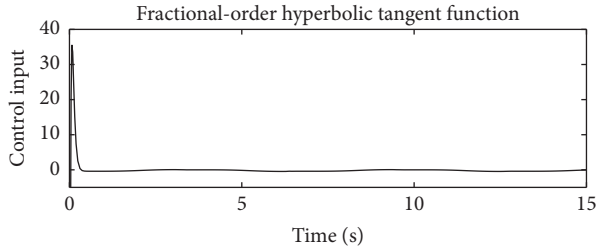


(c)

Figure 11: Controller output diagram.

surface combined with the hyperbolic tangent function can further improve the system's stability.

## 7. Conclusions

The interconnected two-machine power system will have chaotic oscillation characteristics under some certain parameters. By analyzing the dynamic characteristics of the chaotic oscillation power system, the chaotic oscillation parameters are obtained. In order to suppress the chaotic oscillation, the fractional-order hyperbolic tangent sliding mode controller is designed to control the chaotic power system. Simulation results show that the continuous smooth hyperbolic tangent function reduced the chattering phenomenon and the fractional-order sliding surface improved the system control performance. The proposed fractional-order hyperbolic tangent sliding mode controller can suppress the chaotic oscillation and shorten the convergence time of the chaotic power system. The designed controller has the advantages of fast response, good stability, and strong robustness. In the future, the proposed control method of this paper will be applied to other related control fields to improve the control performance.

## Data Availability

The data used to support the findings of this study are available from the corresponding author upon request.

## Conflicts of Interest

The authors declare that they have no conflicts of interest.

## Acknowledgments

This work was supported by the China Postdoctoral Science Foundation (2020M683685XB), Natural Science Basic Research Plan in Shaanxi Province of China (2020JQ-633).

## References

[1] Q. Lu and Y. Z. Sun, *Power System Nonlinear Control*, Science Press, Beijing, China, 1993.

[2] L. Yuan, J. Q. Shen, F. Xiao, and M. L. Chen, "Nonsingular terminal sliding-mode observer design for interior permanant magnet synchronous motor drive at very low-speed," *Acta Physica Sinica*, vol. 62, no. 3, Article ID 30501, 2013.

[3] D. K. Lal and K. S. Swarup, "Modeling and simulation of chaotic phenomena in electrical power systems," *Applied Soft Computing*, vol. 11, no. 1, pp. 103–110, 2011.

[4] Y. H. Qin, X. S. Luo, and D. Q. Wei, "Random-phase-induced chaos in power systems," *Chinese Physics B*, vol. 19, no. 5, Article ID 50511, 2010.

[5] Y. H. Qin and J. C. Li, "Random parameters induce chaos in power systems," *Nonlinear Dynamics*, vol. 77, no. 4, pp. 1609–1615, 2014.

[6] W. D. Zhang and W. N. Zhang, "Analysis of parameters for chaotic power systems," *Power System Technology*, vol. 24, no. 12, pp. 17–20, 2000.

[7] C.-Y. Ma, J.-H. Liu, and C.-L. Wang, "Chaos of a power system model and its control," *Journal of Vibration and Control*, vol. 18, no. 14, pp. 2176–2185, 2012.

[8] H. Gholizadeh, A. Hassannia, and A. Azarfar, "Chaos detection and control in a typical power system," *Chinese Physics B*, vol. 22, no. 1, Article ID 10503, 2013.

[9] S. Y. Dong, H. Bao, and Z. Wei, "Calculations and simulations of the chaotic oscillation threshold in daul-unit systems," *Proceeding of the CSEE*, vol. 20, no. 19, pp. 58–63, 2010.

[10] F. Y. Sun and Q. Li, "Dynamic analysis and chaos of the 4D fractional-order power system," *Abstract Applied Analysis*, vol. 2014, Article ID 534896, 2014.

[11] W. Tan, Z. P. Li, and M. Zhang, "Chaotic oscillation of interconnected power system and its synchronization," *Journal of Hunan University of Science & Technology (Natural Science)*, vol. 26, pp. 74–78, 2011.

[12] D. Zhong, S. G. Gao, H. Zhao, Y. J. Ma, and S. J. Liu, "Controlling chaos in power system based on finite-time stability theory," *Chinese Physics B*, vol. 20, no. 12, Article ID 120501, 2011.

[13] I. M. Ginarsa, A. Soeprijanto, and M. H. Purnomo, "Controlling chaos and voltage collapse using an ANFIS-based composite controller-static var compensator in power systems," *International Journal of Electrical Power & Energy Systems*, vol. 46, pp. 79–88, 2013.

[14] Z. Y. Zhu, W. T. Liu, and L. Y. Cai, "Chaos control of ship electrical power system based on output delay feedback method," *Ship Engineering*, vol. 31, no. 6, pp. 36–40, 2009.

[15] J. Ni, L. Liu, C. Liu, X. Hu, and A. Li, "Chaos suppression for a four-dimensional fundamental power system model using adaptive feedback control," *Transactions of The Institute of Measurement and Control*, vol. 39, no. 2, pp. 194–207, 2017.

[16] J. Zhai and H. R. Karimi, "Universal adaptive control for uncertain nonlinear systems via output feedback," *Information Sciences*, vol. 500, pp. 140–155, 2019.

[17] S. Song, J. H. Park, B. Zhang, X. Song, and Z. Zhang, "Adaptive command filtered neuro-fuzzy control design for fractional-order nonlinear systems with unknown control

directions and input quantization," *IEEE Transactions on Systems, Man, and Cybernetics: Systems, Early Access*, vol. 202, pp. 1–12, 2020.

[18] S. Song, B. Zhang, J. Xia, and Z. Zhang, "Adaptive back-stepping hybrid fuzzy sliding mode control for uncertain fractional-order nonlinear systems based on finite-time scheme," *IEEE Transactions on Systems, Man, and Cybernetics: Systems*, vol. 50, no. 4, pp. 1559–1569, 2020.

[19] F. H. Min, M. L. Ma, W. Zhai, and E. R. Wang, "Chaotic control of the interconnected power system based on the relay characteristic function," *Acta Physica Sinica*, vol. 63, no. 5, Article ID 50504, 2014.

[20] S. M. Jiang, Z. Z. Zeng, and K. Y. Chen, "A new sliding mode control method of chaos control for interconnected power systems," *Control Engineering of China*, vol. 24, no. 5, pp. 978–983, 2017.

[21] G. Gugapriya, P. Duraisamy, A. Karthikeyan, and B. Lakshmi, "Fractional-order chaotic system with hyperbolic function," *Advances in Mechanical Engineering*, vol. 11, no. 8, 2019.

[22] J. K. Ni, C. X. Liu, and X. Pang, "Fuzzy fast terminal sliding mode controller using an equivalent control for chaotic oscillation in power system," *Acta Physica Sinica*, vol. 62, no. 19, Article ID 190507, 2013.

[23] D. R. Zhu, W. C. Zhang, and J. D. Duan, "Hyperbolic function sliding mode control for chaos oscillation in power system," *Journal of Xi'an University of Technology*, vol. 33, no. 2, pp. 220–225, 2017.

[24] J. Ni, L. Liu, C. Liu, X. Hu, and S. Li, "Fast fixed-time nonsingular terminal sliding mode control and its application to chaos suppression in power system," *IEEE Transactions on Circuits and Systems II: Express Briefs*, vol. 64, no. 2, pp. 151–155, 2017.

[25] J. B. Wang, C. X. Liu, Y. Wang, and G. C. Zheng, "Fixed time integral sliding mode controller and its application to the suppression of chaotic oscillation in power system," *Chinese Physics B*, vol. 27, no. 7, Article ID 70503, 2018.

[26] B. Bourouba and S. Ladaci, "Robust fuzzy adaptive sliding mode stabilization for fractional-order chaos," *Algorithms*, vol. 11, no. 7, p. 101, 2018.

[27] S. P. Nangrani and S. S. Bhat, "Numerical study of optimized fractional-order controller for chaos control of nonlinear dynamical power system," *IEEE Transactions on Electrical Energy Systems*, vol. 27, no. 8, Article ID e2336, 2017.

[28] G. Sun, L. Wu, Z. Kuang, Z. Ma, and J. Liu, "Practical tracking control of linear motor via fractional-order sliding mode," *Automatica*, vol. 94, pp. 221–235, 2018.

[29] L. Xiong, J. Wang, X. Mi, and M. W. Khan, "Fractional order sliding mode based direct power control of grid-connected DFIG," *IEEE Transactions on Power Systems*, vol. 33, no. 3, pp. 3087–3096, 2018.

[30] K. Rabah and S. Ladaci, "A fractional adaptive sliding mode control configuration for synchronizing disturbed fractional-order chaotic systems," *Circuits, Systems, and Signal Processing*, vol. 39, no. 3, pp. 1244–1264, 2020.

[31] J. P. Singh and B. K. Roy, "The nature of Lyapunov exponents is (+, +, −, −). Is it a hyperchaotic system?" *Chaos, Solitons & Fractals*, vol. 92, pp. 73–85, 2016.

[32] J. P. Singh and B. K. Roy, "The simplest 4-D chaotic system with line of equilibria, chaotic 2-torus and 3-torus behaviour," *Nonlinear Dynamics*, vol. 89, no. 3, pp. 1845–1862, 2017.

[33] J. P. Singh and B. K. Roy, "A more chaotic and easily hardware implementable new 3-D chaotic system in comparison with 50 reported systems," *Nonlinear Dynamics*, vol. 93, no. 3, pp. 1121–1148, 2019.

[34] I. Podlubny, *Fractional Differential Equations*, Academic Press, San Diego, CA, USA, 1999.

[35] D. Matignon, "Stability results for fractional differential equations with applications to control processing," *Computational Engineering in Systems Applications*, vol. 2, pp. 963–968, 1996.

[36] J. B. Hu, Y. Han, and L. D. Zhao, "A novel stablility theorem for fractional systems and its applying in synchronizing fractional chaotic system based on back-stepping approach," *Acta Physica Sinica*, vol. 58, no. 4, pp. 2235–2239, 2009.

[37] C. M. Qin, N. M. Qi, and K. Zhu, "State space modeling and stability theory of variable fractional order system," *Control and Decision*, vol. 26, no. 11, pp. 1757–1760, 2011.

[38] M. M. Polycarpou and P. A. Loannou, "Modelling, identification and stable adaptive control of continuous-time nonlinear dynamical systems using neural networks," *Proceedings of the American Control Conference*, vol. 1, pp. 36–40, 1992.

[39] A. I. Petros and J. Sun, *Robust Adaptive Control*, Prentice-Hall, Englewood Cliffs, NJ, USA, 1996.

[40] J. P. Singh and B. K. Roy, "Crisis and inverse crisis route to chaos in a new 3-D chaotic system with saddle, saddle foci and stable node foci nature of equilibria," *Optik*, vol. 127, no. 24, pp. 11982–12002, 2016.